



Effect of submerged vegetation density on flow under favorable pressure gradient

Mahboobeh Brahimi¹ · Hossein Afzalimehr²

© Springer Nature Switzerland AG 2018

Abstract

Many species of flexible submerged vegetation are observed in natural streams in which the flow is rarely uniform. For better understanding the effect of flexible submerged vegetation density on the flow, experiments were conducted in the Hydraulics Laboratory of Isfahan University of Technology, Iran. Two runs with grassy artificial weeds with high and low density and one run without vegetation as a base case under favorable pressure gradient (FPG) flow were considered. Results showed the distributions of drag coefficient vary along vegetation strip. For both vegetation densities from bed to $z/H = 0.6$, the velocity profile trend was like that in emergent vegetation. This result could be inferred from the low degree of vegetation submergence. The Reynolds shear stress showed a wavy distribution at both submerged vegetation densities under FPG flow. The maximum and minimum values of Reynolds shear stress were more in dense vegetation than in sparse one. In addition, results revealed turbulence intensity depend not only on FPG flow, but also on the vegetation density.

Keywords Submerged vegetation · Favorable pressure gradient (FPG) · Drag coefficient · Vegetation density · Reynolds shear stress

List of symbols

The following symbols are used in this paper

\underline{A}	projected plant area perpendicular to flow
A_i	mean frontal vegetal area
A^*	the advection term
a	vegetation density
C_d	vegetal drag coefficient
d_{50}	median grain size
d_{16}	16% finer particle diameters
d_{84}	84% finer particle diameters
g	gravitational acceleration
H	water of depth
h	vegetation bending height
L	length of channel in which n was counted
L_{veg}	length of vegetation along the flume
n	number of plants in area of ($W * L$)

P^*	the pressure term
Re_d	vegetal Reynolds number
S_r	degree of submergence
S^*	the bed slope effect term
$\langle U \rangle$	double averaging velocity
$\langle uw \rangle$	Reynolds stress at the vegetation edge
$(-u'w')$	Reynolds shear stress
$\left(\sqrt{(u')^2} / u_* \right)$	dimensionless stream-wise turbulence intensity
u	stream-wise velocity component
u'	velocity fluctuation in longitudinal direction
U	mean velocity
U_*^2	Reynolds stress at the vegetation edge
u^*	shear velocity:
V	vegetation volume
w'	Velocity fluctuation in vertical direction

✉ Hossein Afzalimehr, hafzali@cc.iut.ac.ir; Mahboobeh Brahimi, m.brahimi@ag.iut.ac.ir | ¹Water Engineering Department, Isfahan University of Technology, Isfahan, Iran. ²Department of Civil Engineering, Iran University of Science and Technology, Tehran, Iran.

$\left(\sqrt{(w')^2}/u_*\right)$	dimensionless vertical turbulence intensity
W	channel width
z	distance from the bed
σ_g	Geometric standard deviation
λ	dimensionless vegetation density
δ	height from bed in which maximum velocity occurred

1 Introduction

The favorable pressure gradient (FPG) flow, in which the depth of flow decreases and velocity increases in the flow direction, has been reviewed frequently [1–9]. Studies in open channels with bare banks and coarse-bed indicate that the favorable pressure gradient flow suppresses the generation of turbulence [9]. In recent years, many researches have been conducted in vegetated streams due to the significant role played by vegetation in erosion, sediment transport and resistance to flow. Review of literature reveals that there are many studies on submerged vegetation [10–12] and flexible vegetation [13, 14]. Some researchers mentioned that the maximum Reynolds stress and turbulence intensity occurred approximately at the deflected vegetation height [15–18]. Wu et al. developed a method to estimate the vegetal drag coefficient (C_d) for emergent and submerged vegetation under uniform flow [19]. They showed that the significant factors for drag coefficient were Reynolds number, height of vegetation, and slope. They also reported that there was a direct relation between slope and vegetal drag coefficient when the Reynolds number was held constant. Järvelä investigated the effects of some factors on drag coefficient and found that there were large variations with velocity, depth of flow, Reynolds number, and vegetal morphology [14]. For example, they showed the vegetal drag coefficient for the leafy willows was three to seven times that of the leafless willows. Fathi-Moghadam and Kouwen showed the drag coefficient was changing due to plant bending against flow and with changing in the mean flow velocity [20]. The momentum absorbing area changes with bending submerged vegetation, so they demonstrated there is a good agreement between friction factor and flow velocity. Most researchers consider a constant drag coefficient for the whole flow depth, however, Rowinski et al. and Murphy et al. used different drag coefficients changing with depth of water [21, 22]. Nepf showed that the additional drag generated by vegetation reduces velocity within vegetation and increases depth of flow [23]. The more residence time of water above the vegetated elements leads to more

infiltration into the vegetated root zone and in long run, benefit the vegetation [24–26].

Wang et al. showed there is significant bias between imaged and modeled water surface profile $H(x)$ [27]. This difference motivated the empirical analysis of the drag coefficient which is dependent on the stream-wise direction in order to be used in the Saint-Venant equations. They suggested that drag coefficient must be varying along vegetation length in stream-wise direction. Their finding illustrated that $C_d(x)/\langle C_d \rangle$ increases and then decreases with increasing distant from flume inlet forming a hump-shape that has been studied elsewhere [28]. The drag coefficient for dense vegetation differs from that of single vegetation of the same form. The different vegetation density means different Reynolds number (Re_d). Therefore, for achieving the value of drag coefficient closest to the real condition, the group of vegetation should be considered [29]. The sheltering role has a great effect on the effective friction factor or Manning roughness value which is used in different equations. The sheltering effect occurs when the Reynolds number was sufficiently high ($Re_d \gg 1000$); as a consequence, additional wake is produce by rod canopy.

Most of the studies used solid circular cylinders in regular rows for quantifying the impact of vegetation on flow characteristics and drag coefficient [28–33]. However, cylinders do not adequately represent vegetation because of the differences in flexibility, roughness, shape, etc. It is worth saying there is no comprehensive theoretical description for flexible vegetation therefore the theoretical formulation for rigid vegetation is used for flexible vegetation with some reservation [34]. Some researcher tried to present quantitative way to describe plant flexibility. For instance, Kouwen and Unny used plastic strips for simulating submerged flexible vegetation and represented a way in which the elasticity of vegetation were used as to describe plant flexibility [35]. They used values of mEI to show flexibility in which m is plant density, E is elasticity and I is stem area's second moment of inertia. However, many researchers argue against this idea due to difficulties for measuring elasticity, lacking of any physical concept or variations in modulus of elasticity [29, 36].

The FPG flow with presence of a vegetation strip is frequently seen over gravel and cobble bed; however, to our knowledge, no study has been reported on flow structure in the presence of a vegetation strip under FPG flow. Graf and Altinakar, Song and Chiew [37] showed that the stream-wise turbulent intensity component is concave at bare bank condition under FPG flow. This study aimed to show the effects of different submerged vegetation densities on drag coefficient, velocity profiles, Reynolds stress and turbulent intensity distributions which are necessary

in hydraulic modelling, especially for evaluating the drag force, sediment transport and aquatic habitat. Besides, the low submergence degree of vegetation makes it possible to compare the results with emergent vegetation.

2 Theoretical and experimental modeling

Experiments were conducted in an 8 m long, 0.4 m wide, 0.6 m deep flume with total discharge capacity of 50 l/s in the Hydraulics Laboratory of Isfahan University of Technology, Iran. The flume was rectangular with glassed walls. The depth of water was set 20 cm by tailgate at the end of the flume. To produce FPG flow with a slope of -1.5% the cobble particles were arranged carefully along the flume. Cobble particles were used for this study, because natural vegetation protrudes often from cobble bed (Fig. 1). The bottom slope of rivers is usually positive

as rivers flow downward. However, there are cases when the slope may be locally negative (adverse), forcing the water to flow over a rising bottom. From fluvial hydraulic point of view, flow over stoss side of dunes in sand-bed rivers and flow from deep section (pool) to shallow region (riffle) in gravel-bed rivers are good examples to show the favorable pressure gradient flow.

The median grain size of cobble-bed was determined by the Wolman method [38], $d_{50} = 52.5$ mm, and the geometric standard deviation $\sigma_g = (d_{84}/d_{16})^{0.5}$ of the particle size distribution was 1.18, where d_{84} and d_{16} were 84% and 16% finer particle diameters, respectively (Fig. 2). To fill the space between cobbles, smaller particles of gravel were used.

All data were collected from the sections of 5.5, 6, 6.5 and 6.75 m of the flume entrance, where flow was fully developed and any possible effects of entrance or tailgate were minimized.

Fig. 1 The scheme of flume and used instruments

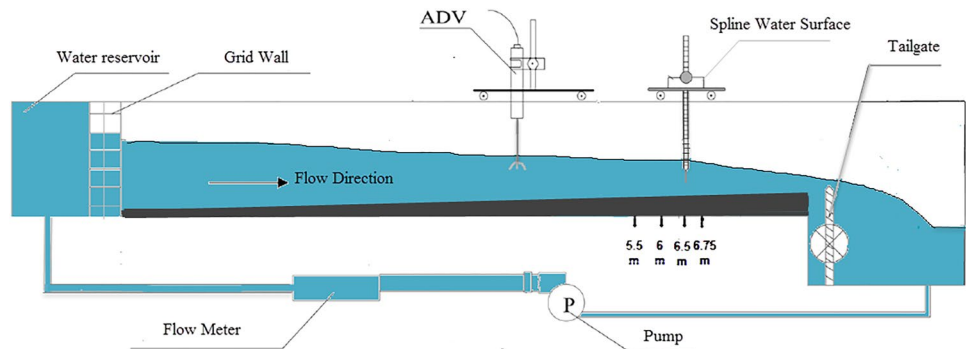
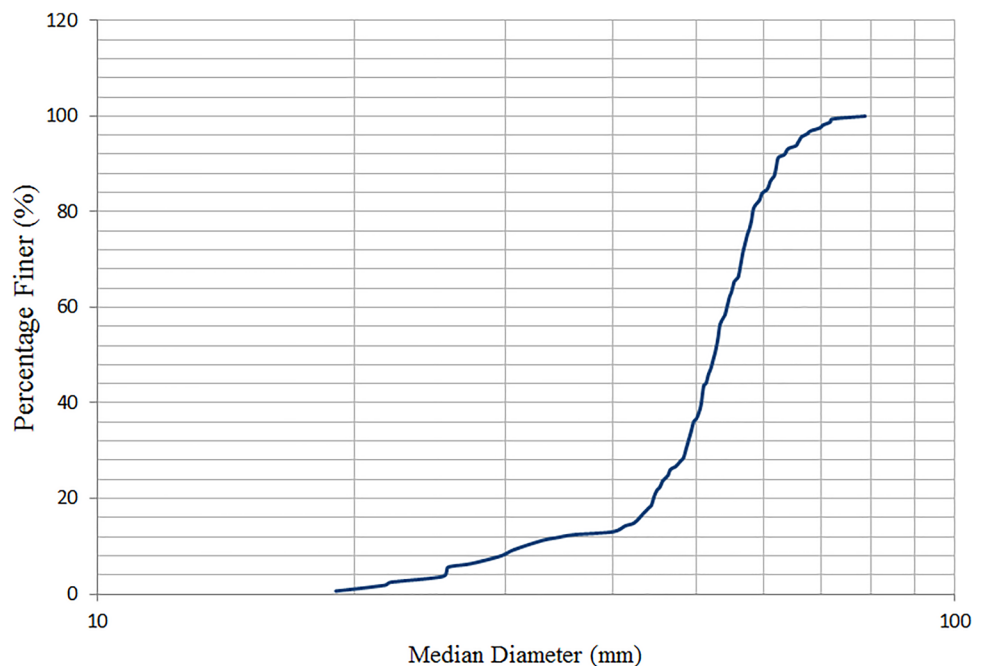


Fig. 2 Grain size distribution in the flume



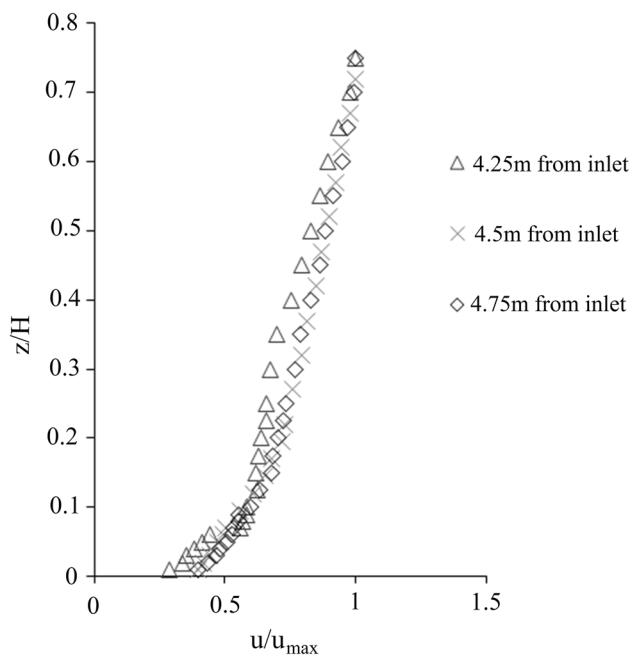


Fig. 3 Self-similar of velocity profiles near section of 4.5 m from inlet

To prove the uniform flow is fully developed, the velocity profiles have to be self-similar at different distances from the flume entrance. At present study, the fully developed flow occurs at a distance of 4.5 m downstream from the flume entrance (Fig. 3).

A down looking Acoustic Doppler velocimetry (ADV), 10 MHz Nortek Vectrino, was used to measure the instantaneous three-dimensional velocity components. ADV record instantaneous velocity components at a single-point with a relatively high frequency. Using WinADV and data filtering, measurement sensitivity analysis was performed and then the results was presented. In addition, the variation of duration, frequency of measurements were investigated to check their effects on the results. Accordingly, the high quality data were presented in this study. The used ADV at this study has the precision of $\pm 0.1 \text{ mm s}^{-1}$ and a sampling volume with a height of 5.5 mm. To present the correct data, the following criteria were considered: signal to noise ratio larger than 15, coefficient of correlation higher than 90 percent and spectral analysis [39]. The Explore V software package was used for post-processing of measured velocity records, including removal of sporadic spikes with acceleration and velocity threshold filters. The phase-space threshold despiking technique appears to be a robust method in steady flows [40, 41]. At each measuring point, 24,000 velocity data were collected. After post-processing method, between 10 to 20% of all samples were removed.

Two runs of measurements were carried out with different plant densities and one run was measured without vegetation as a base case. Each velocity profile consists of twenty-point velocities. The fluctuating turbulence near channel bed is more important than that of near water surface. Therefore the velocity measurements in vertical spacing (vertical distance between two consecutive points for measuring point velocity) was chosen as 2, 5 and 10 mm from the vicinity of the channel bed to the water surface.

At present study, the vegetation was flexible and was bended under flow. In these situations, the connectivity of the mesh is accompanied by error. The mesh was located in random position, so the values of operation may not be correct and mesh free method was used.

To investigate the influence of morphology and density of flexible vegetation on flow structure, grassy artificial weeds with densities of 0.162 and 0.243 were used. These densities were selected based on inspiration from some natural vegetation strip in Kaj River. The selected artificial vegetation is similar to the morphology of the common aquatic vegetation growing in cobble-bed rivers. The number of vegetation plants was evaluated by counting vegetation plants in $2 \text{ m} \times 0.13 \text{ m}$. The vegetation strip had a 0.13 m width and 8 m length along the flume. The selected artificial plants were deflected below the water surface. This vegetation embedded randomly between holes of cobbles at 1/3 of the flume width, so the 13 cm width of bed from the right vertical wall along the flume was covered with a submerged vegetation strip (Fig. 4). Some of measured hydraulic data are given in Table 1. The degree of submergence was defined as the rate of depth of water to vegetation bending height ($S_r = H/h$). The degree of submerged vegetation was 1.235 and 1.143, thus it was possible to investigate flow characteristics with emergent vegetation conditions. As above was mentioned, measuring the exact deflected vegetation height is very difficult task. All vegetation elements do not bend uniformly, therefore, average deflected height should be presented. The vegetation used at this study has the width of 8 mm at the bottom and 2 mm at the top. However, average width of each element was considered 7 mm. Vegetation were embedded randomly in a 13-cm width strip. For parameter of ΔS , which is an average center-to-center vegetation distance, authors assumed uniform center to center distance.

The definition of Reynolds number for flexible vegetation is not constant and several options have been suggested [42, 43]. In the present study the multiplication of stem thickness in bending vegetation height was consider as a frontal vegetal area (A_c) (Table 1):

$$A_c = \text{bending vegetation height}(m) \times \text{width of vegetation element}(m) \tag{1}$$

and Reynolds number is defined as:

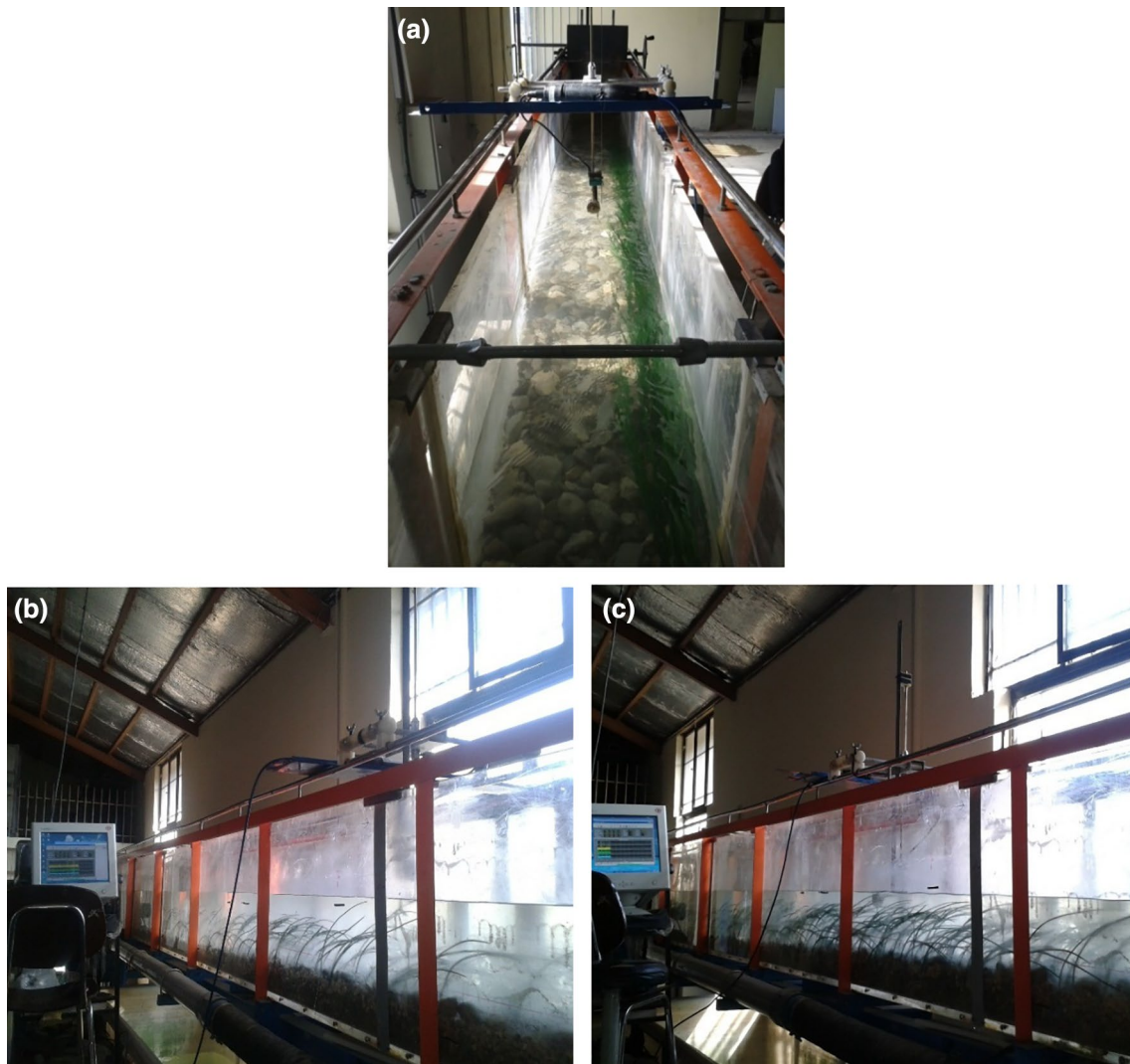


Fig. 4 a top view of vegetation strip in the flume, b low vegetation density under FPG flow, c high vegetation density under FPG flow

Table 1 A summary of experimental data

Run	λ	Thickness (mm)	Median length (m)	Bending length (m)	Width (m)	u_{max} (cm/s)	u_* (cm/s)	S_r	Re_d
High dense	0.243	0.001	0.283	0.162	0.007	42.88	3.81	1.235	10763
Low dense	0.162	0.001	0.283	0.175	0.007	39.94	2.95	1.143	11339

$$Re_d = \frac{U\sqrt{A_c}}{\nu} \tag{2}$$

in which U is mean velocity, A_c is frontal vegetal area and ν is the kinematic viscosity of water.

The vegetation density $a [m^{-1}]$ was determined by dividing the projected plant area perpendicular to flow by the vegetation volume (Eq. (3)) as:

$$a = \frac{A}{V} = \frac{n\bar{A}_i}{WhL} \tag{3}$$

where n is the number of plants in area of ($W * L$), W is the channel width, \bar{A}_i is the mean frontal vegetal area, h is the vegetation bending height, and L is the length of channel in which n was counted. In the present study the frontal vegetal area was considered constant with increasing depth of flow, because the stem shape of vegetation almost had the same surface from the top to the bottom. To express the vegetation density with a dimensionless factor, the vegetation density was written as $\lambda = a * h$. Vegetation density is one of important factors for resistance to flow but it is difficult to obtain it for flexible plants which are placed irregularly.

The measurements of velocity was done near vegetation strip (2 cm away from vegetation strip). The ADV probes do not act very well into the branches of vegetation, therefore all measurements was done outside the vegetation strip. In this way, the influences of interaction of braches are more important compared to connection between branches of the modeling.

Wang et al. showed that conventional formulation of drag coefficient for isolated and a group of cylinders cannot exactly predict the water surface profile [27]. They introduce new formulation for drag coefficient by substituting the S_f (Eq. 4) into SVE (Eq. 5):

$$S_f = \frac{C_d m D U^2}{(1 - \lambda) 2g} \tag{4}$$

$$U \frac{\partial U}{\partial x} + g \frac{\partial H}{\partial x} - g(S_0 - S_f) = 0 \tag{5}$$

$$C_d = (1 - \lambda) \frac{\Delta S^2}{D L_{veg}} (S_0^* + P^* - A^* - R^*) \tag{6}$$

in above equations S_f is energy grade line slope, g is gravitational acceleration, m is the number of vegetation stems per unit ground area, D is interpreted as the frontal width of the vegetation stem, S_0 is the bed slope, ΔS is an average center-to-center vegetation distance, S_0^* is bed slope effect term, P^* is pressure term, A^* is advection term and R^* is rainfall term that present study is no-rainfall case.

$$S_0^* = S_0 \left(\frac{L_{veg}}{U^2 / 2g} \right) \tag{7}$$

$$P^* = \left(-\frac{\partial H}{\partial x} \right) \left(\frac{L_{veg}}{U^2 / 2g} \right) \tag{8}$$

$$A^* = \left(\frac{\partial U}{\partial x} \right) \left(\frac{2L_{veg}}{U} \right) \tag{9}$$

3 The results and discussion

As above was mentioned, measuring the exact deflected vegetation height is very demanding. All vegetation elements do not bend uniformly, therefore, average deflected height should be presented. The vegetation used at this study has the width of 8 mm at the bottom and 2 mm at the top. However, average width of each element was considered 7 mm. Vegetation were embedded randomly in a 13-cm width strip. For parameter of ΔS , which is an average center-to-center vegetation distance, authors assumed uniform center to center distance.

3.1 Drag Coefficient

The distributions of drag coefficient derived from Eq. 6 have been shown in Fig. 5. As can be seen from the graph, drag coefficient changes along vegetation strip. Previous studied showed that drag coefficient vary in flow depth [21], besides, the result of present study show that drag coefficient vary along vegetation strip that is in good agreement with Wang et al. and Wang et al. [27, 28]. At high dense vegetation case, the drag coefficient increase with increasing x along the vegetation stream, however, at 6.5 m from inlet, a slight drop has been observed. In contrast, the trend of drag coefficient at low dense vegetation was decreasing. It might have increasing trend before 5.5 m from inlet, however, there is no evident data to prove it.

3.2 Velocity profiles

Figure 6 shows velocity profiles at the same position for different vegetation densities. At these profiles, the velocity in the longitudinal direction was normalized by the maximum velocity in that direction; also the distance

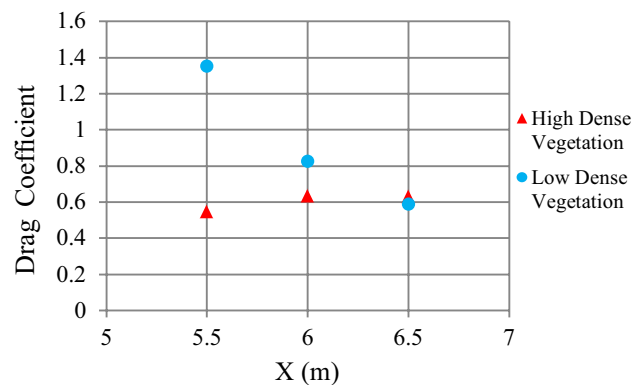


Fig. 5 Drag coefficient profiles near vegetation strip at high and low vegetation densities along the flume

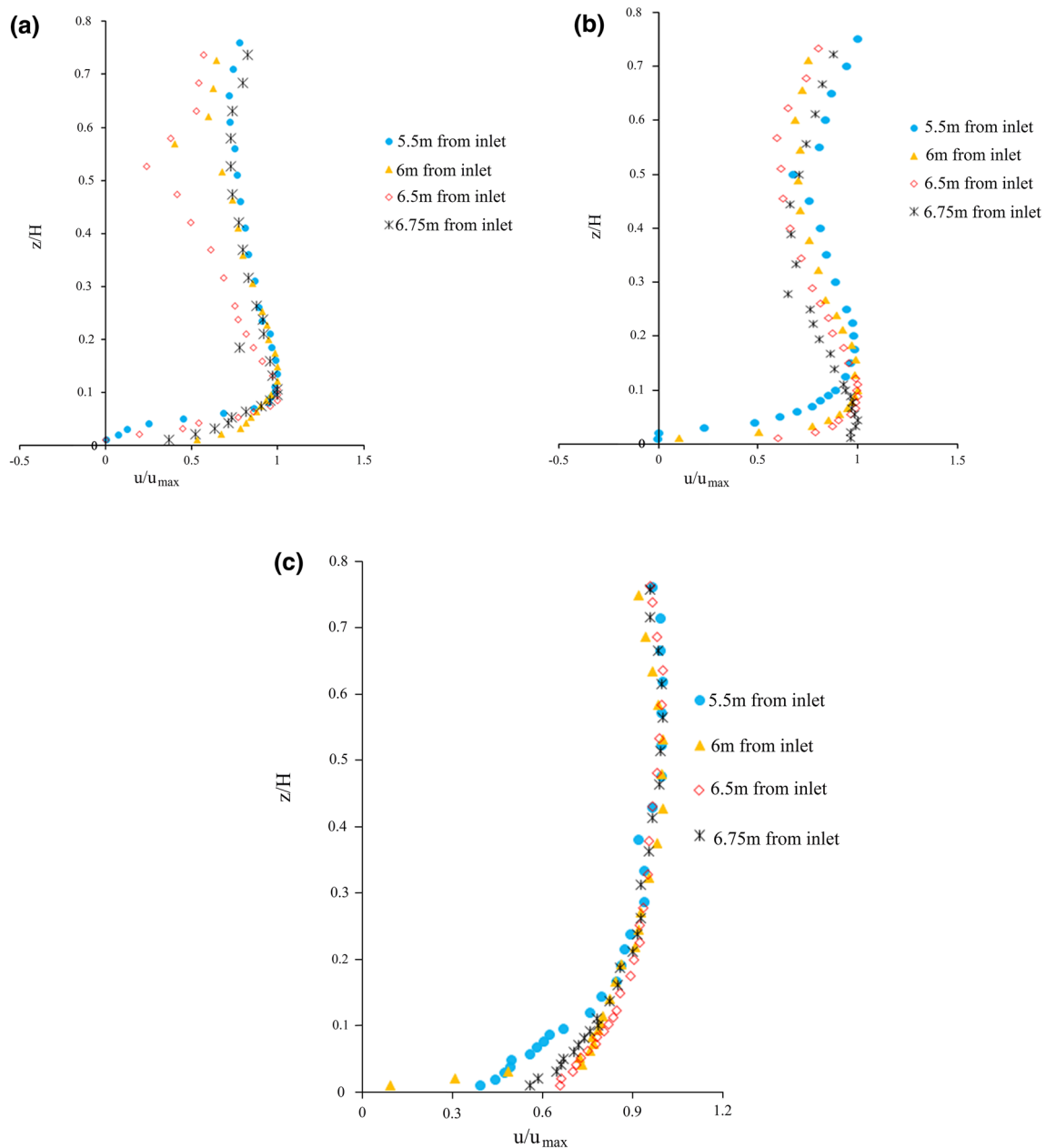


Fig. 6 Comparison of dimensionless stream-wise velocity distribution near vegetation density: **a** High dense vegetation, **b** Low dense vegetation, **c** Bare bank

from the bed (z), which it was showed on the vertical axis, normalized by the maximum depth of water (H). The figure shows the velocity distribution in both vegetation densities was S shaped [5], while at bare banks as a base case the velocity distribution was convex and the maximum stream-wise velocity occurred under the water surface. As in 1989, Nezu et al. said all channels with $W/H < 5$ were considered as a narrow channel [44]. The maximum flow velocity in the narrow channel occurs under the water surface: ($\delta < H$) where δ is the height from bed in which

maximum velocity occurred. The importance of this phenomenon is that the effects of walls and secondary current are sensible. Just as shown on graphs, the velocity profile was divided into three layers. In the first layer, velocity increased from the bed up to $z/H = 0.1$ and this was due to the friction force prevailing in the flow direction. In the first layer near cobble bed, the values of velocity in dense vegetation were lower than sparse vegetation (Fig. 6a, 6b). In the other words, velocity distribution near cobble bed starts at lesser values ($0 < u < 0.5$ cm/s), but in lower density

this values starts at a higher rate ($0 < u < 1$ cm/s) and this is due to more resistance to flow in dense vegetation. In the second zone, from $z/H = 0.1$ to $z/H = 0.6$, the velocity had a decreasing trend. In this zone two or three stems on each plant created more resistance against the flow. A decreasing trend was more sensible in dense vegetation than in sparse one and this was due to more stems and increasing resistance to flow, therefore creating a significant wake zone on the back of stems. This wake zone is more sensible in 6 m and 6.5 m from inlet in dense vegetation. In the third zone from $z/H = 0.6$ up to the water surface, the velocity profile had an increasing trend. In this zone, due to no attendance of vegetation, the increasing trend was predictable. In both modes of submerged vegetation density from bed to $z/H = 0.6$ the velocity profile trend was just like as in emergent vegetation [45]. This result can be gained from the low degree of vegetation submergence ($H/h = 1.235, 1.143$). On other hand, the existence of vegetation with low degree of submergence caused the velocity profile for submergence vegetation to be like the velocity profile for emergent vegetation and only the difference was the third zone near water surface. The velocity increased in this zone, however, velocity distribution in emergent vegetation only had first and second zones. The presence of layer without any vegetation near the water surface in submerged vegetation created less wake zone and more mixing than in emergent one. The changes in bed roughness and relative submergence (H/d_{50}) due to the combination of cobble and vegetation produced an S-shape profile. However, the vegetation density and flow conditions around the vegetation modify the profile shape, showing a steep or a mild increasing trend in the third layer near the water surface.

3.3 Reynolds Stress

Reynolds shear stress ($-\overline{u'w'}$) is one of the most important parameters for understanding flow characteristics. As Fig. 7 shows, the Reynolds shear stress was made dimensionless by the square of shear velocity (u_*^2). Yang et al. mentioned that the presence of non-zero vertical velocity (w) in non-uniform flow deflected the Reynolds shear stress distribution from a linear trend [46]. Figure 7 shows a wavy distribution for Reynolds shear stress in both submerged vegetation density under favorable pressure gradient (FPG) flow, supporting the findings of Afzalimehr et al. [4, 5]. Afzalimehr et al. [4] found that the nonlinear distribution of Reynolds stress is due to secondary currents and the anisotropy in turbulence in the vegetated banks channels [4].

The maximum and minimum values of Reynolds shear stress were more in dense vegetation than in sparse one. In the layer near water surface where vegetation did not

exist, the value of Reynolds shear stress was generally positive. A decreasing trend of the distribution of stress near the bed was observed and that was in agreement with Afzalimehr et al. [5]. The maximum value of Reynolds shear stress occurred near the cobble bed. Based on Figs. 6 and 7, where the Reynolds shear stress came to zero is the point where the velocity reaches the maximum value. Also, the interaction of vegetation and cobble produces a three-layer distribution with negative values in $z/H < 0.4$. Figures 6a and 6b illustrate that in the "middle veg layer" the velocity reduces due to vegetation resistance. In Fig. 7a and 7b the values of $-\overline{u'w'}$ are negative in the middle layer, showing an upward vertical transport of momentum with negative velocity gradients [47]. The negative Reynolds stresses in regions with different velocity gradients (see Fig. 6) may be formed by some localized regions where the energy of turbulence is transferred to the mean flow as reported by Siniscalchi and Nikora [48]. Figure 7c shows that the Reynolds stress distribution follows the classic form (a convex form) for bare bank case. For bare bank flow the maximum Reynolds stress occurred at the bed (6.5 m and 6.75 m from inlet), thereafter it decreased to free water surface. Reynolds stress reached zero value at around $z/H = 0.65$ and then recorded the negative value near water surface. In 5.5 m and 6 m from inlet the maximum Reynolds stress occurred away from the bed that is in agreement with Afzalimehr findings [1]. It is clear the trend of Reynolds stress deviates from linear distribution that is in agreement with Stone and Hotchkiss [49]. They say this deviation is because of large roughness elements in the bed.

3.4 Turbulence intensities

Creating of turbulence is due to the velocity component fluctuations, which causes momentum transport between different fluid layers. The turbulence can be quantitative by Reynolds stress and turbulence intensity. Turbulence intensity is a major factor affecting on erosion, sediment transport, flow resistance and creating different bed forms [50].

Figure 8 shows the distribution of stream-wise turbulent intensity ($\sqrt{(u')^2}/u_*$) and vertical turbulent intensity ($\sqrt{(w')^2}/u_*$) near vegetation strip. As the figure shows the stream-wise turbulent intensity component is concave at bare bank condition under FPG flow. This result confirms the results of Graf and Altinakar, Song and Chiew and Afzalimehr [1, 37]. The stream-wise turbulent intensity remained concave with the presence of low dense vegetation, except for 6.75 m from inlet in which this distribution turned to convex pattern. The reason of this change might be the presence of strong secondary currents and effects

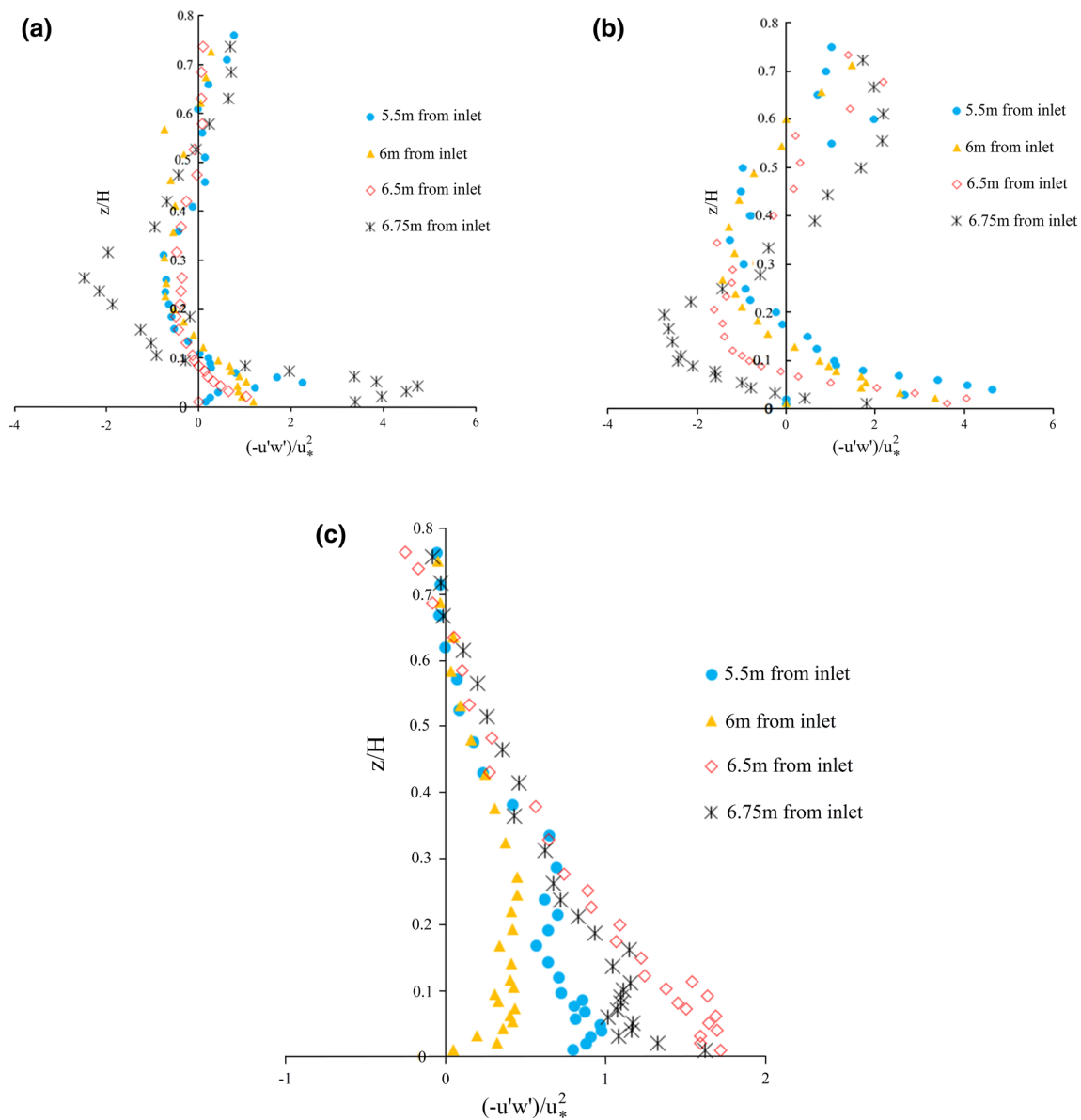


Fig. 7 Comparison of dimensionless shear stress distributions under FPG flow near vegetation strip: **a** High vegetation density, **b** Low vegetation density, **c** Bare bank

of vegetation. The maximal value of turbulent intensity of $(\sqrt{(u')^2}/u_*)$ was located near bed. However, in 6.75 m from inlet, the maximum value of stream-wise turbulence intensity was observed at vegetation bending height. The distribution stream-wise turbulent intensity in high dense of vegetation is totally different compared to bare bank and low dense vegetation. The turbulent intensities of $(\sqrt{(u')^2}/u_*)$ at four different cross sections did not follow the same pattern, and generally they were wave-shaped.

The vertical turbulent intensity $(\sqrt{(w')^2}/u_*)$ in bare bank and low dense of vegetation was almost constant

from bed up to water surface, however, this parameter in high dense vegetation has decreased at inner layer and then remain constant up to water surface. A number of previous experimental and numerical studies have concluded that turbulent intensities reduce in the inner layer [9]. In addition, in high dense vegetation, the value of turbulence intensity is greater than sparse one.

The value of turbulent intensity in longitudinal and vertical directions at present study was more than previous studies [1]. This can be attributed to presence of cobbles and large roughness elements.

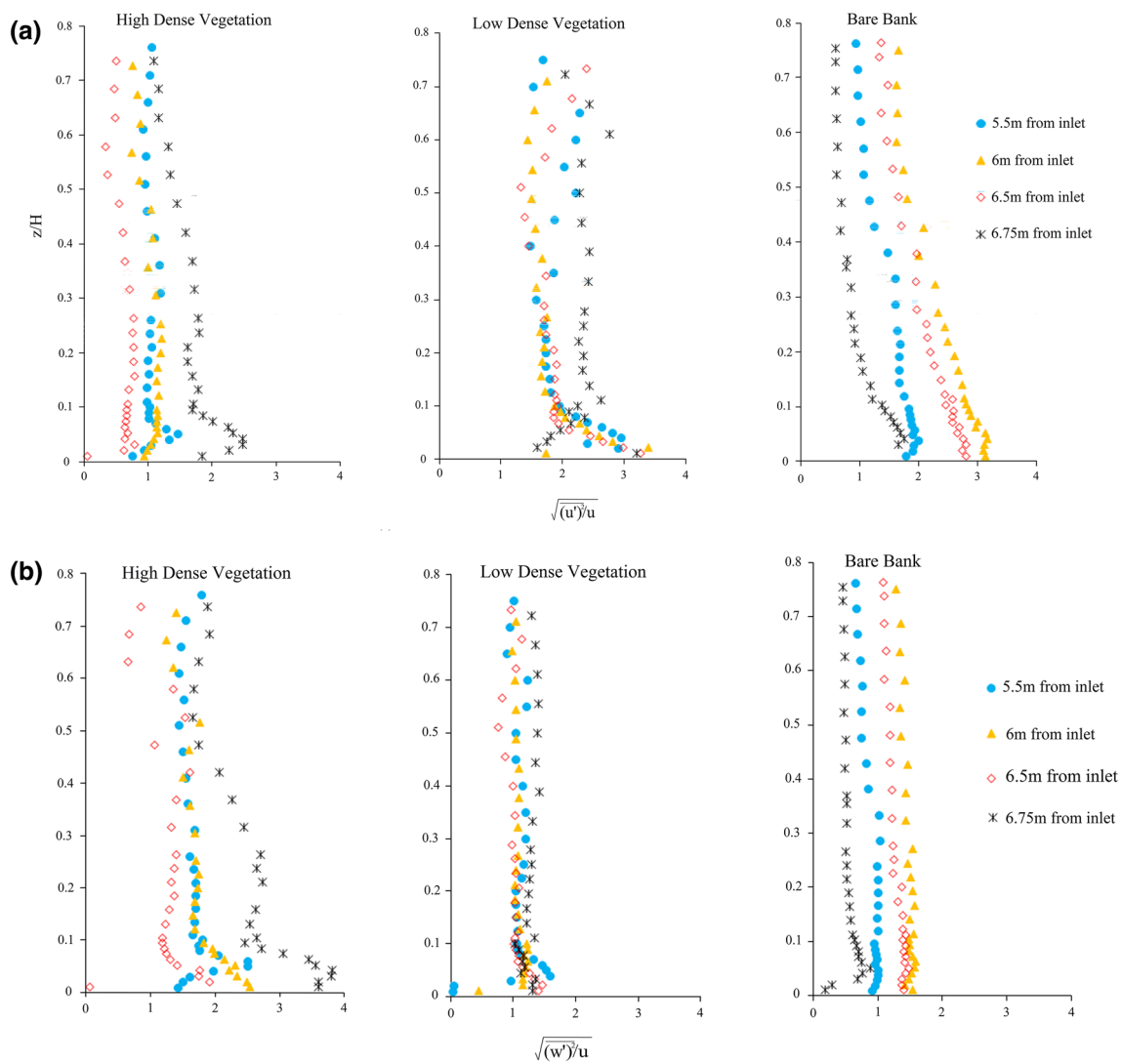


Fig. 8 Turbulence intensity at high dense vegetation, low dense vegetation and bare bank **a** longitudinal direction **b** vertical direction

3.5 The conclusion

In the present study, the effect of artificial submerged vegetation density under favorable pressure gradient (FPG) flow is investigated, and the following results were achieved:

The drag coefficient distributions vary along vegetation strip at both vegetation densities. At high dense vegetation, this trend was increasing and then decreasing, however, at low dense vegetation this trend was decreasing.

The velocity profile trends in both submerged artificial vegetation densities from bed to $z/H = 0.6$ were just like those emergent vegetation. This result can be gained from the low degree of vegetation submergence ($H/h = 1.235, 1.143$). On other hand, the presence of vegetation with low degree of submergence causes the

velocity profile to be similar to that in emergent vegetation; the only difference is the presence of third zone near the water surface in the submergence case, but the velocity increased in this zone, however, the emergent vegetation velocity profiles only had first and second zones. The presence of layer without any vegetation near the water surface in submerged vegetation resulted in the creation of less wake zone and more mixing than in emergent vegetation. Near-bed velocity starts at lesser value in high dense vegetation compared to low dense vegetation due to more resistance to flow in dense vegetation.

A wavy distribution for Reynolds shear stress (RSS) in both submerged vegetation densities under FPG flow was observed, while for the bare bank, profiles deviate from linear distribution, that is because of large roughness elements in the bed. The values of Reynolds shear stress were generally positive near the cobble bed, but the interaction

of cobble-vegetation leads to values in middle layer of the RSS distribution. Near-bed Reynolds stress starts at more value in dense vegetation compared to low dense vegetation due to more resistance to flow in dense vegetation. In some cases in bare bank, maximum Reynolds stress occurred away from the bed.

The stream-wise turbulence intensity follows concave pattern at bare bank and with the presence of low density of vegetation. However, as the vegetation density increase, this pattern has changed into almost wavy shape. The vertical turbulence intensity remained constant up to water surface at bare bank and low vegetation density. Although, in the presence of high vegetation density, considerable scatters are observed in vertical turbulent intensity. It can be concluded that turbulence intensity depend not only on the FPG flow, but also on the vegetation density.

The FPG flow, submerged vegetation strip and cobble bed can be found in nature easily, however, rivers are complex system and the result of laboratory flume should extend for rivers carefully. Although, previous study by Afzalimehr et al. [51] showed that there is considerable similarity between flume and river velocity profiles, Reynolds shear stress and correlation coefficient. This helps to better interpret the laboratory results for extending to field works.

Acknowledgements The authors appreciate the efforts by Isfahan University of Technology for preparing this manuscript.

Compliance with ethical standards

Conflict of interest On behalf of all authors, the corresponding author states that there is no conflict of interest.

References

- Afzalimehr H (2010) Effect of non-uniformity of flow on velocity and turbulence intensities in flow over a cobble-bed. *J Hydrol Process* 24(3):331–341
- Maddahi MR, Afzalimehr H, Rowinski PM (2016) Flow characteristics over a gravel bedform: Kaj River case study. *J Acta Geophys* 64(5):1779–1796
- Fazel E, Afzalimehr H, Sui J (2017) A comparison of two-dimensional and three-dimensional flow structures over artificial pool-riffle sequences. *Can J Civ Eng*. <https://doi.org/10.1139/cjce-2017-0274>
- Afzalimehr H, Fazel E, Singh VJ (2010) Effect of vegetation on banks on distributions of velocity and Reynolds stress under accelerating flow. *J Hydro Eng Am Soc Civil Eng (ASCE)* 15(9):708–713
- Afzalimehr H, Fazel E, Gallichand J (2012) Effects of accelerating and decelerating flows in a channel with vegetated banks and gravel bed. *Int J Sed Res* (27):188–200
- Song T, Graf WH (1994) Nonuniform open-channel flow over a rough bed. *JHHE* 12(1):1–25
- Kironoto B, Graf WH (1995) Turbulence characteristics in rough nonuniform open-channel flow. *Proc ICE Water Maritime Energy* 112:316–348
- Cardoso AH, Graf WH, Gust G (1991) Steady gradually accelerating flow in a smooth open channel. *J Hydraul Res Delft, The Netherlands* 29(4):525–543
- Houra T, Tsuji T, Nagano Y (2000) Effects of adverse pressure gradient on quasi-coherent structures in turbulent boundary layer. *Int J Heat Fluid Flow* 21:304–311
- Afzalimehr H, Moghbel R, Sui J (2011) Hydraulic parameters in channels with wall vegetation and gravel bed. *Int J Sed Res* 25:81–90
- Nepf HM, Ghisalberti M (2008) Flow and transport in channels with submerged vegetation. *Acta Geophys* 56(3):753–777
- Sukhodolov A N, Sukhodolova T A (2006) Evolution of mixing layers in turbulent flow over submerged vegetation: field experiments and measurement study, paper presented at the Internatl. In: Conf. on Fluvial Hydraulics (River Flow), 6–8 September 2006, Lisbon, Portugal
- Ghisalberti M, Nepf HM (2006) The structure of the shear layer in flows over rigid and flexible canopies. *Environ Fluid Mech* 6:277–301
- Järvelä J (2005) Effect of submerged flexible vegetation on flow structure and resistance. *J Hydrol* 307(1):233–241
- Nezu I, Sanjou M (2008) Turbulence structure and coherent motion in vegetated open-channel flows. *J Hydro Environ Res* 2:62–90
- Ghisalberti M, Nepf HM (2009) Shallow flows over a permeable medium: the hydrodynamics of submerged aquatic canopies. *Transp Porous Media* 78:385–402
- Carollo FG, Ferro V, Termini D (2002) Flow velocity measurements in vegetated channels. *J Hyd Eng* 128:664–673
- Jarvella J (2004) Flow resistance in environmental channels: focus on vegetation. Degree of Doctor of Science, Helsinki University of Technology, Helsinki
- Wu FC, Shen HW, Chou YJ (1999) Variation of roughness coefficients for unsubmerged and submerged vegetation. *Hydraul Eng* 125(9):934–942
- Kouwen N, Fathi-Moghadam M (2000) Friction factors for coniferous trees along rivers. *J Hydraul Eng* 126(10):732–740
- Rowinski PM, Kubrak E, Kubrak J (2002) Vertical velocity distribution through and above submerged, flexible vegetation. *Hydrol Sci J* 53(4):905–920
- Murphy E, Ghisalberti M, Nepf H (2007) Model and laboratory study of dispersion in flows with submerged vegetation. *Water Resour Res* 43:W05438
- Nepf HM (1999) Drag, turbulence, and diffusion in flow through emergent vegetation. *Water Resour Res* 35:479–489
- Rietkerk M, Boerlijst MC, van Langevelde F, HilleRisLambers R, van de Koppel J, Kumar L, Prins HH, de Roos AM (2002) Self-organization of vegetation in arid ecosystems. *Am Nat* 160(4):524–530. <https://doi.org/10.1086/342078>
- Thompson S, Katul G, Konings A, Ridolfi L (2011) Unsteady overland flow on flat surfaces induced by spatial permeability contrasts. *Adv Water Resour* 34(8):1049–1058. <https://doi.org/10.1016/j.advwatres.2011.05.012>
- Assouline S, Thompson S, Chen L, Svoray T, Sela S, Katul G (2015) The dual role of soil crusts in desertification. *J Geophys Res Biogeosci* 120(10):2108–2119. <https://doi.org/10.1002/2015JG003185>
- Wang W-J, Huai W-X, Thompson S, Peng W-Q, Katul GG (2017) Drag coefficient estimation using flume experiments in shallow non-uniform water flow within emergent vegetation during rainfall. *Ecol Indic*. <https://doi.org/10.1016/j.ecolind.2017.06.041>

28. Wang W-J, Huai W-X, Thompson S, Katul GG (2015) Steady nonuniform shallow flow within emergent vegetation. *Water Resour Res* 51:10047–10064. <https://doi.org/10.1002/2015WR017658>
29. Wilson CAME (2007) Flow resistance models for flexible submerged vegetation. *J Hydrol* 342:213–222
30. Finnigan J (2000) Turbulence in plant canopies. *Annu Rev Fluid Mech* 32:519–572
31. Poggi D, Porpotato A, Ridolfi L (2004) The effect of vegetation density on canopy sub-layer turbulence. *Bound Layer Meteor* 111:565–587
32. Tanino Y, Nepf HM (2008) Laboratory investigation of mean drag in a random array of rigid, emergent cylinders. *J Hydraul Eng.* [https://doi.org/10.1061/\(ASCE\)0733-9429\(2008\)134:1\(34\)](https://doi.org/10.1061/(ASCE)0733-9429(2008)134:1(34))
33. Nicolle A, Eames I (2011) Numerical study of flow through and around a circular array of cylinders. *J Fluid Mech* 679:1–31
34. Kutija V, Hong HTM (1996) A numerical model for assessing the additional resistance to flow introduced by flexible vegetation. *J Hydraul Res* 34(1):99–114
35. Kouwen N, Unny T (1973) Flexible roughness in open channels. *J Hydraul Div 99 ASCE* 99:713–728
36. Fischenich C (2000) Resistance due to vegetation. EMRRP Technical Notes, ERDC TNEMRRP-SR-07, Us Army Engineer Research and Development Center, Vicksburg, MS
37. Afzalimehr H, Barahimi M, Sui J (2017) Non-uniform flow over cobble bed with submerged vegetation strip. In: *Proceedings of the ICE- water management*, pp 1–16
38. Wolman MG (1954) A method of sampling coarse river bed material, *Trans. AGU* 35(6):951–956
39. Garcia CM, Cantero MI, Nino Y, Garcia MH (2005) Turbulence measurements with acoustic doppler velocimeters. *J Hydraul Eng ASCE* 131(12):1062–1073
40. Wahl TL (2003) Despiking acoustic doppler velocimeter data. Discussion. *J Hydraul Eng ASCE* 129(6):484–487
41. Chanson H, Trevethan M, Aoki S (2008) Acoustic doppler velocimetry (ADV) in small estuary: field experience and signal post-processing. *Flow Meas Instrum* 19(5):307–313. <https://doi.org/10.1016/j.flowmeasinst.2008.03.003>
42. Vogel S (1994) *Life in moving fluids*. Princeton Univ. Press, Princeton, p 467
43. Statzner B, Lamouroux N, Nikora V, Sagnes P (2006) The debate about drag and reconfiguration of freshwater macrophytes: comparing results obtained by three recently discussed approaches. *Freshwater Biol* 51:2173–2183. <https://doi.org/10.1111/j.1365-2427.2006.01636.x>
44. Nezu I, Nakagawa H, Rodi W (1989) Significant difference between secondary currents in closed channels and narrow open channel. In: *The 23rd IAHR congress*, Ottawa, Canada, pp. 125–132
45. Nepf HM, Vivoni ER (2000) Flow structure in depth-limited, vegetated flow. *J Geophys Res* 105:28547–28557
46. Yang SQ, Xu WL, Yu GL (2006) Velocity distribution in a gradually accelerating free surface flow. *Adv Water Resour* 29:1969–1980
47. Siniscalchi F, Nikora VI, Aberle J (2012) Plant patch hydrodynamics in streams: mean flow, turbulence, and drag force. *Water Resour Res* 48(1):1513
48. Siniscalchi F, Nikora VI (2012) Flow-plant interactions in open-channel flows: a comparative analysis of five freshwater plant species. *Water Resour Res* 48:W05503. <https://doi.org/10.1029/2011WR011557>
49. Stone MC, Hotchkiss R (2007) Turbulence description in two cobble-bed river reaches. *J Hydraul Eng* 133(12):1367–1378
50. Carollo FG, Ferro V, Termini D (2005) Analyzing turbulence intensity in gravel bed channel. *J Hyd Eng ASCE* 131:1050–1061
51. Graf WH, Altinakar MS (1998) *Fluvial hydraulics, flow and transport processes in channels of simple geometry*. Wiley, New York, p 681